Correlation induced spin freezing transition in FeSe: a dynamical mean field study

Ansgar Liebsch[1] and Hiroshi Ishida[2]

[1] *Institut für Festkörperforschung, Forschungszentrum Jülich, 52425 Jülich, Germany*
[2] *College of Humanities and Sciences, Nihon University, Tokyo 156, Japan*

The effect of local Coulomb interactions on the electronic properties of FeSe is explored within dynamical mean field theory combined with finite-temperature exact diagonalization. The low-energy scattering rate is shown to exhibit non-Fermi-liquid behavior caused by the formation of local moments. Fermi-liquid properties are restored at large electron doping. In contrast, FeAsLaO is shown to be located on the Fermi-liquid side of this spin freezing transition.

The recent discovery of high-temperature superconductivity in iron-based pnictides [1] and chalcogenides [2] has led to an intense discussion concerning the role of Coulomb correlations in these materials. Although compounds such as FeAsLaO (1111), BaFe$_2$As$_2$ (122), LiFeAs (111), and FeSe (11) all have rather similar one-electron properties, a variety of experiments suggest significant differences. For instance, photoemission measurements show that FeAsLaO is moderately correlated, with about 50 % 3d band narrowing and effective mass enhancement of about 2 to 3 [3]. In contrast, several photoemission data on FeSe$_x$Te$_{1-x}$ samples reveal larger effective mass enhancement and stronger band narrowing [4–8], optical measurements exhibit incoherent spectral features indicative of a pseudogap [9], and several transport measurements show large deviations from Fermi-liquid behavior [10–13]. Moreover, recent theoretical work [14] suggests that Coulomb interactions in (11) compounds ought to be less well screened than in (1111) systems.

The aim of this paper is to elucidate the origin of the experimentally observed bad-metallic behavior of FeSe. Using an accurate single-particle description of the electronic structure together with appropriate interaction parameters [14], and evaluating the influence of local Coulomb interactions within dynamical mean field theory (DMFT) [15], we show that correlations are strong enough to give rise to the formation of Fe 3d local moments, implying non-Fermi-liquid behavior, where electronic states at the Fermi energy exhibit a finite lifetime. Moreover, we demonstrate that these properties are caused by a nearby doping-driven spin-freezing transition, i.e., Fermi-liquid behavior is restored towards larger electron doping, whereas hole doping reinforces bad-metallic properties. Using the same approach for FeAsLaO we show that Coulomb interactions are too weak to cause spin freezing, so that this system merely exhibits moderate effective mass enhancement [16].

Thus, FeSe appears to be a material which exhibits bad-metallicity induced by a spin freezing transition, a mechanism recently identify by Werner *et al.* [17] in a three-band model. For FeAsLaO, Haule *et al.* [18] showed that large Coulomb interactions lead to the formation of local moments and large scattering rates, while Ishida and Liebsch [19] discussed the spin freezing transition as a function of Coulomb interaction and doping. Bad-metallic behavior in FeSe was also found in DMFT studies by Craco *et al.* [20] and Aichhorn *et al.* [21]. The spin-freezing origin of this behavior, however, was not investigated in these works.

To account for local Coulomb interactions among Fe 3d electrons we use exact diagonalization [22] (ED) which we have recently extended to five orbitals [19]. Discretization of the lattice surrounding the local impurity is achieved by using ten bath levels, which yields excellent projections of the lattice Green's function onto the cluster consisting of impurity plus bath. Because of the very large size of the Hilbert space of this 15 level system (the largest spin sector has dimension $\sim 40 \times 10^6$) the spacing of excited states is very small so that finite size errors are greatly reduced. Moreover, ED has the advantage of allowing for rotationally invariant Hund exchange. This is of crucial importance for the spin freezing transition since omission of spin-flip and pair-exchange interactions leads to a significant shift of the Fermi-liquid to non-Fermi-liquid phase boundary. For computational reasons we restrict ourselves to the lowest excited states, which are relevant near the $T \to 0$ limit. Only the paramagnetic phase is considered. Further calculational details can be found in Ref. [19].

The electronic properties of FeSe are formulated in terms of the effective low-energy model recently derived by Miyake *et al.* [14]. In this scheme, standard band structure calculations within the local density approximation (LDA) were carried out, analogous to previous work in Refs. [23, 24]. From these results, maximally localized Wannier functions were constructed for the Fe 3d bands, following the procedure discussed in Ref. [25]. The inter-site transfer integrals are then derived from the matrix elements of the Kohn-Sham Hamiltonian $H(\mathbf{k})$ in the basis of these Wannier functions. Finally, the constrained random-phase-approximation (RPA) developed by Aryasetiawan *et al.* [26] was used to determine the effective Coulomb and exchange interaction parameters, which account for screening via Se 4p orbitals. Because
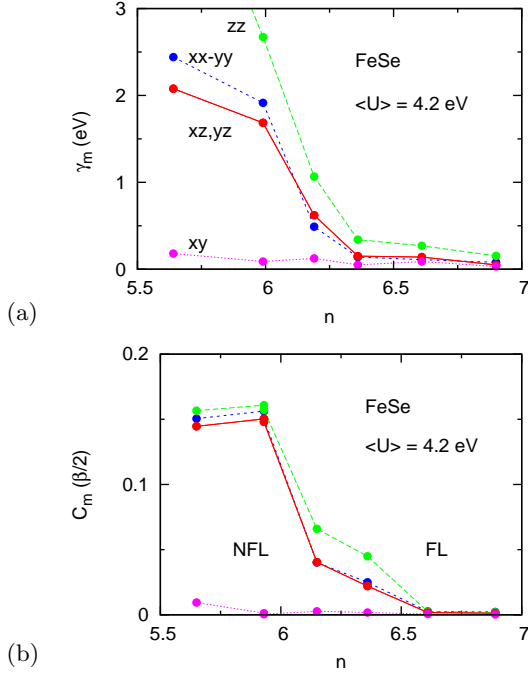
(a)

(b)

FIG. 1: (Color online) (a) Low-energy scattering rates and (b) spin-spin correlations of FeSe as functions of $3d$ occupancy. Near $n = 6$, the non-Fermi-liquid (NFL) behavior $\gamma_m > 0$ is caused by the formation of local moments. Increasing electron doping restores Fermi-liquid (FL) properties, whereas hole doping enhances bad-metallic behavior.

FIG. 2: (Color online) Fe $3d$ orbital occupancies as functions of chemical potential. n_{av} denotes the average occupancy. Nominal occupancy $n = 6$ is reached near $\mu = 17$ eV, while at $\mu = 15$ eV all bands are approximately half-filled.

of the planar structure of FeSe, these screening processes affect the various $3d$ orbitals differently so that the interaction parameters exhibit appreciable orbital dependence. According to these results, the key feature of FeSe is that Coulomb interactions are typically 50% larger than in FeAsLaO. This follows from the larger z spacing and concomitant smaller spread of Wannier orbitals, and from the reduced number of screening channels in FeSe. The one-electron transfer integrals $t_{mn}(\mathbf{R})$ and interaction matrices U_{mn} and J_{mn} for FeSe are given in Tables VII and VIII of Ref. [14], respectively. The average intra-orbital Coulomb interaction is $\langle U \rangle = 4.2$ eV and the average Hund exchange is $\langle J \rangle = 0.5$ eV. The x, y axes point along Fe second-neighbor directions.

Fig. 1(a) shows the low-energy limit of the $3d$ self-energy components, $\gamma_m = -\text{Im} \Sigma_m(i\omega_n \to 0)$, as a function of Fe $3d$ occupancy. The one-electron transfer integrals and interaction matrix elements are kept fixed at the values for $n = 6$. Ordinary Fermi liquid behavior is found for $n > 6.5$, but increasing low-energy scattering rates are obtained at lower electron doping, except for the d_{xy} orbital. Even stronger scattering occurs on the hole doping side, $n < 6$. The reason for the different behavior of γ_{xy} is that $\rho_{xy}(\omega)$ is about 0.5 eV wider than the other density of states components [14].

To identify the origin of this change from Fermi-liquid to non-Fermi-liquid behavior we have evaluated the
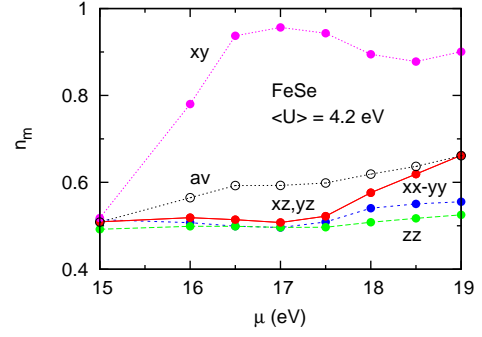
spin-spin correlation function $C_m(\tau) = \langle S_{mz}(\tau) S_{mz}(0) \rangle$, where τ denotes imaginary time. In the case of a Fermi-liquid, these functions decay with τ, so that $C_m(\tau = \beta/2)$ is very small ($\beta = 1/T = 100$ eV^{-1}). The susceptibilities $\chi_m \sim \int_0^\beta d\tau \langle S_{mz}(\tau) S_{mz}(0) \rangle$ then are Pauli-like, i.e., independent of temperature. Fig. 1(b) shows that the results for $n > 6.5$ are consistent with this behavior. At smaller electron doping, the $C_{m \neq xy}(\tau)$ components reach increasingly larger constant values near $\tau = \beta/2$. The corresponding susceptibilities χ_m then become proportional to $1/T$, as expected for Curie-Weiss behavior.

A similar spin-freezing transition was recently found by Werner $et\ al.$ [17] for a degenerate three-band model near $n = 2$, i.e., at one electron away from half-filling. Using continuous-time quantum Monte Carlo DMFT, the paramagnetic phase at moderate U was shown to exhibit Fermi-liquid properties at small n. For $n > 1.5$, an incoherent metallic phase appears, where the self-energy exhibits a finite onset at $\omega = 0$ due to the formation of local moments. Because of particle-hole symmetry, the same Fermi-liquid to non-Fermi-liquid transition appears on the electron-doped side, i.e., when reducing the occupancy below $n \approx 4.5$.

Fig. 2 shows the $3d$ orbital occupancies as a function of doping. At $n = 6$, these values differ significantly from their uncorrelated values: $n_{xz,yz,x^2-y^2,xy,z^2} = (0.54, 0.54, 0.56, 0.60, 0.76)$, indicating strong interorbital charge transfer induced by Coulomb interactions. In particular, n_{xy} reaches nearly unity, while the other n_m are close to half-filling. Despite this orbital polarization, the spectral distributions (not shown here) reveal considerable intensity near E_F, suggesting that the system is not in a Mott phase, where one of the subbands is filled and the others are split into lower and upper Hubbard bands. These kinds of partial Mott transitions, with certain subbands empty or full, are found in several three-band t_{2g} materials, such as LaTiO$_3$ [27, 28], V$_2$O$_3$ [29, 30], and Ca$_2$RuO$_4$ [31, 32].

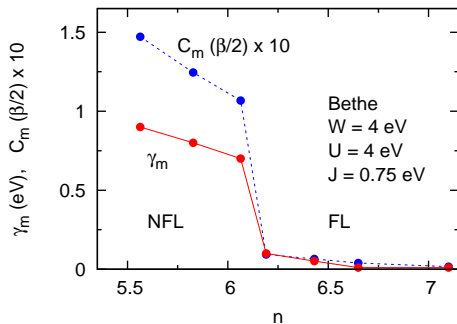To investigate the relationship between orbital polar-

FIG. 3: (Color online) Low-energy scattering rates and spin-spin correlations derived within ED/DMFT for a degenerate five-band model with Bethe lattice density of states with $W = 4$ eV. For $U = 4$ eV, $J = 0.75$ eV, the spin-freezing transition occurs at $n = 6.2$, with Fermi-liquid behavior at $n > 6.2$ and increasing bad-metallicity for $n < 6.2$. For $U = 4$ eV, $J = 0.5$ eV (not shown), the transition occurs at $n = 6.1$.

ization and local moment formation, we have calculated the effect of Coulomb correlations in a fully degenerate five-band model consisting of identical densities of states for a Bethe lattice, with band width and Coulomb interactions of similar magnitude as in FeSe. As shown in Fig. 3, this model system exhibits the same kind of spin-freezing transition as discussed above for FeSe. For $n = 6$, the low-energy scattering rate indicates non-Fermi-liquid behavior, associated with the formation of local moments. Fermi-liquid behavior is recovered at electron doping $n > 6.2$, whereas hole doping strengthens bad-metallic properties. The important conclusion from this result is that orbital polarization is not a prerequisite for the spin-freezing transition. Thus, this picture differs from the orbital-selective, itinerant-localized scenarios proposed in Refs. [33–36].

To understand better to what extent the results for FeSe shown in Fig. 1 depend on the details of the single-particle Hamiltonian, we have carried out analogous ED/DMFT calculations by replacing $H(\mathbf{k})$ with the tight-binding Hamiltonian derived by Graser et $al.$ for FeAsLaO [37]. Since the $3d$ density of states components of this compound are qualitatively similar to those of FeSe, there ought to be also a spin-freezing transition. Indeed, if we retain the FeSe interaction parameters with an average Coulomb energy of 4.2 eV, the overall behavior of the low-energy scattering rates γ_m and spin-spin correlations C_m are qualitatively similar to the ones shown in Fig. 1, except for a less pronounced orbital polarization. For instance, at $n = 6$, $n_{xy} = 0.77$ rather than 0.95. Nevertheless, the Fermi-liquid to non-Fermi-liquid transition also occurs near $n = 6.5$, suggesting that this phenomenon is remarkably robust, i.e., insensitive to the details of the one-electron properties. These results further support the key point of the degenerate-band example presented in Fig. 3, namely, that the spin freezing
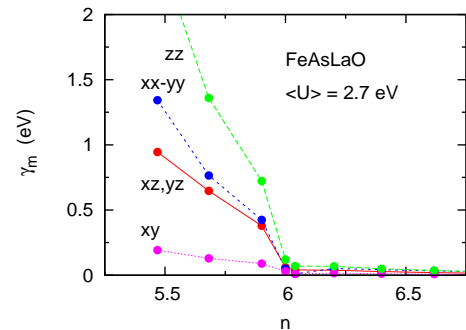
(a)
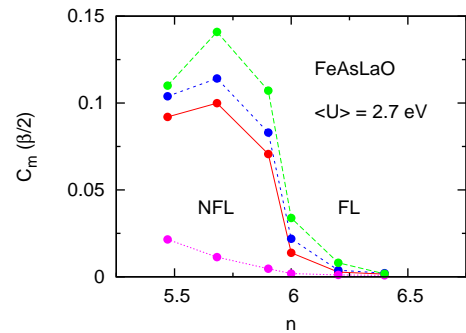
(b)

FIG. 4: (Color online) (a) Low-energy scattering rates and (b) spin-spin correlations of FeAsLaO as functions of $3d$ occupancy. The Fermi-liquid to non-Fermi-liquid transition caused by local moment formation occurs close to $n = 6$. Electron doping maintains Fermi-liquid properties, whiles hole doping leads to bad-metallic behavior.

transition is not driven by orbital polarization.

According to the work by Miyake et $al.$ [14], the crucial difference between FeSe and FeAsLaO is that, because of more efficient dp screening and more extended Wannier orbitals, local Coulomb interactions in the latter system are considerably smaller, with $\langle U \rangle \approx 2.7$ eV and $\langle J \rangle \approx 0.4$ eV. In previous ED/DMFT calculations for FeAsLaO [19] based on orbital independent Coulomb and exchange energies we showed that spin freezing may occur at about $U = 3$ eV for Hund exchange $J = 0.75$ eV. Using the recently published orbital dependent U_{mn} and J_{mn} matrices derived within constrained RPA [14], we are now able to make a more accurate prediction of the spin freezing transition in FeAsLaO. The transfer integrals and interaction parameters are again held fixed at their values for $n = 6$. As shown in Fig. 4, the transition now is located almost exactly at $n = 6$. Thus, in contrast to FeSe, Fermi-liquid properties in FeAsLaO prevail and the $3d$ bands exhibit only moderate effective mass enhancement, $m^* \approx 2 \dots 3$ [16]. Nonetheless, hole doping $n < 6$ gives rise to local moment formation and bad-metallic behavior, with a finite lifetime at E_F, while electron doping stabilizes the Fermi-liquid properties. (Note the weaker orbital polarization compared to the results for FeSe in Fig. 1. Also, because of orbital dependent U_{mn}, J_{mn}, the magnitudes of γ_m and $C_m(\beta/2)$ differ from those for orbital independent U, J in Ref. [19].)
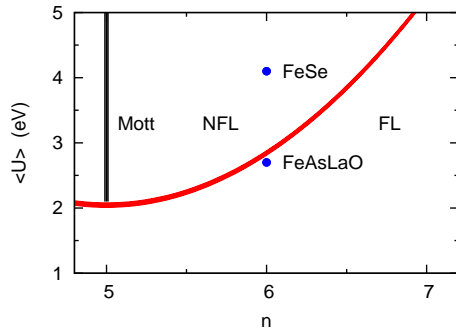
FIG. 5: (Color online) Schematic phase diagram for FeSe and LaFeAsO. Solid curve: spin freezing transition indicating the boundary between Fermi-liquid and non-Fermi-liquid phases. Vertical bar at half-filling: Mott insulating phase.

On the basis of these results we arrive at the phase diagram depicted in Fig. 5. FeSe is located well inside the non-Fermi-liquid phase, whereas FeAsLaO lies on the Fermi-liquid side of the spin-freezing transition. Both systems exhibit 'parent' Mott phases in the limit $n = 5$.

We finally discuss the role of spin-flip and pair-exchange interactions. In Ref. [19] it was shown that the omission of these terms in the many-body impurity treatment leads to a significant shift of the Fermi-liquid to non-Fermi-liquid phase boundary to ~ 1 eV smaller $\langle U \rangle$. Thus, for FeSe bad-metallic behavior would become even stronger. Since FeAsLaO, however, lies very close to the phase boundary, this approximation has severe consequences. Instead of a Fermi-liquid characterized by moderate effective mass enhancement, this compound is then also bad-metallic, in conflict with experiments.

The present work is based on a consistent combination of single-particle Hamiltonian, constrained RPA interaction parameters, and DMFT many-electron calculations within a 5×5 d electron basis. It would be interesting to compare the spin freezing transition obtained within this scheme to analogous formulations within a pd electron basis, such as the one used in Ref. [21].

In summary, we have evaluated the effect of local correlations in FeSe, using accurate single-particle properties and constrained RPA results for the orbital dependent Coulomb and exchange matrices, combined with ED/DMFT. The finite scattering rates derived from the $3d$ components of the self-energy are shown to be linked to the formation of local moments. Thus, FeSe is bad-metallic, in agreement with experimental findings. Spin freezing ceases for large electron doping, giving rise to Fermi-liquid behavior. In contrast, hole doping enhances bad-metallicity. Applying the same scheme to FeAsLaO we find that, as a result of the more efficiently screened Coulomb interactions, local moment formation is confined to hole doping $n < 6$. Thus, FeAsLaO and FeSe

seem to be located on opposite sides of the Fermi-liquid to non-Fermi-liquid spin freezing transition.

[1] Y. Kamihara, T. Watanabe, M. Hirano, and H. Hosono, J. Am. Chem. Soc. **130**, 3296 (2008).
[2] F. C. Hsu *et al.*, Proc. Natl. Acd. Sci. USA **105**, 14262 (2008).
[3] W. Maleb *et al.*, J. Phys. Soc. Jpn. **77**, 093714 (2008).
[4] R. Yoshida *et al.*, J. Phys. Soc. Jpn. **78**, 034708 (2009).
[5] A. Yamasaki *et al.*, arXiv:0902.3314 (unpublished).
[6] Y. Xia *et al.*, Phys. Rev. Lett. **103**, 037002 (2009).
[7] K. Nakayama *et al.*, arXiv:0907.0763 (unpublished).
[8] A. Tamai *et al.*, arXiv:0912.3152 (unpublished).
[9] G. F. Chen *et al.*, Phys. Rev. B **79**, 140409(R) (2009).
[10] I. Pallechi *et al.*, Phys. Rev. B **80**, 214511 (2009).
[11] M. Tropeano *et al.*, arXiv:0912.0395 (unpublished).
[12] Y.J. Song *et al.*, arXiv:0911.2045 (unpublished).
[13] B. C. Scales *et al.*, Phys. Rev. B **79**, 094521 (2009).
[14] T. Miyake *et al.*, J. Phys. Soc. Jpn. **79**, 044705 (2010).
[15] A. Georges *et al.*, Rev. Mod. Phys. **68**, 13 (1996).
[16] M. Aichhorn *et al.* found similar results for Ising exchange: Phys. Rev. B **80**, 085101 (2009).
[17] P. Werner *et al.*, Phys. Rev. Lett. **101**, 166405 (2008).
[18] K. Haule, J. H. Shim, and G. Kotliar, Phys. Rev. Lett. **100**, 226402 (2008); K. Haule and G. Kotliar, New. J. Phys. **11**, 025021 (2009).
[19] H. Ishida and A. Liebsch, Phys. Rev. B **81**, 054513 (2010).
[20] L. Craco, M. S. Laad, and S. Leoni, arXiv:0910.3828 (unpublished).
[21] M. Aichhorn *et al.*, arXiv:1003.1286 (unpublished).
[22] M. Caffarel and W. Krauth, Phys. Rev. Lett. **72**, 1545 (1994).
[23] A. Subedi *et al.*, Phys. Rev. B **78**, 134514 (2008).
[24] K.-W. Lee *et al.*, Phys. Rev. B **78**, 174502 (2008).
[25] I. Souza *et al.*, Phys. Rev. B **65**, 035109 (2001).
[26] F. Aryasetiawan *et al.*, Phys. Rev. B **70**, 195104 (2004).
[27] E. Pavarini *et al.*, Phys. Rev. Lett. **92**, 176403 (2004).
[28] A. Liebsch, Phys. Rev. B **77**, 115115 (2008); H. Ishida and A. Liebsch, Phys. Rev. B **77**, 115350 (2008).
[29] G. Keller *et al.*, Phys. Rev. B **70**, 205116 (2004).
[30] A. Liebsch, H. Ishida, and J. Merino, Phys. Rev. B **78**, 165123 (2008).
[31] A. Liebsch and H. Ishida, Phys. Rev. Lett. **98**, 216493 (2007).
[32] E. Gorelov *et al.*, arXiv:1001.4705 (unpublished).
[33] J. Wu *et al.*, Phys. Rev. Lett. **101**, 126401 (2008).
[34] A. Hackl and M. Vojta, New J. Phys. **11**, 055064 (2009).
[35] S.-P. Kou *et al.*, EuroPhys. Lett. **88**, 17010 (2009).
[36] L. de' Medici, S. R. Hassan, and M. Capone, J. Supercond. Nov. Mat. **22**, 535 (2009).
[37] S. Graser *et al.*, New. J. Phys. **11**, 025016 (2009).